To cite this article: YAN H, ZHOU G H. Measurement of ship's magnetization parameters based on Kalman filtering method[J/OL]. Chinese Journal of Ship Research, 2022, 17(4). http://www.ship-research.com/en/article/doi/10.19693/j.issn.1673-3185.02273.

DOI: 10.19693/j.issn.1673-3185. 02273

Measurement of ship's magnetization parameters based on Kalman filtering method

YAN Hui[1], *ZHOU Guohua*[*2]

1 College of Big Data and Artificial Intelligence, Xinyang University, Xinyang 464000, China

2 College of Electrical Engineering, Naval University of Engineering, Wuhan 430033, China

Abstract: [**Objectives**] This study proposes a measurement scheme based on the Kalman filtering method for improving efficiency and lowering complexity in measuring the magnetization parameters of shipboard three-component geomagnetic field measurement systems. [**Methods**] The principles and characteristics of magnetization in the mathematical model of a shipboard three-component geomagnetic field measurement system are studied. The steps for applying the Kalman filtering algorithm are used to compute the ship's magnetization parameters. Then, computer simulation and mockup experiment are conducted to testify its validity. [**Results**] The simulation and experiment show that the three-component geomagnetic field can be computed precisely, and the algorithm performs well in convergence with a small sampling of data. [**Conclusions**] Therefore, the Kalman filtering method has higher efficiency and lower cost in the practice of measuring a ship's magnetization parameters.

Key words: three-component geomagnetic field; ship's magnetic field; Kalman filtering; magnetic silencing

CLC number: U665.26; TM153.1

0 Introduction

Ferromagnetic objects placed in the Earth's magnetic field, such as naval ships, tanks, vehicles, and aircraft, can produce a magnetizing field due to the action of the geomagnetic field [1]. Thus, the magnetic sensor mounted on a ship will be subjected to interference from the ship's magnetizing field. The separation of the three-component geomagnetic field from the measurement data of magnetic sensors is a core issue faced by shipboard geomagnetic field measurement systems. Shipboard degaussing systems are marine equipment that compensates for the ship's magnetizing field with a three-component geomagnetic field as a system control signal [2]. In this system, a three-component magnetic sensor after anti-interference adjustment is mounted on the mast of a naval ship to monitor the geomagnetic field in real time, so as to control the current of the degaussing winding to compensate for the ship's magnetic field, namely, "measuring the geomagnetic field and then degaussing the ship." The purpose of the anti-interference adjustment is to eliminate the interference of the ship's magnetizing field with a geomagnetic measurement sensor.

For eliminating the interference of the ship's magnetizing field with a geomagnetic measurement sensor, it is necessary to measure the ship's induced magnetization parameter matrix and fixed magnetization parameter vector [3] in advance. Depending on the mathematical model of a shipboard three-component geomagnetic field measurement system, Xiao [4] proposed the "four-heading method." However, this method can only be used to measure the elements in the first two columns of the induced magnetization parameter matrix and requires sup-

Received: 2021－01－21 **Accepted**: 2021－08－16

Supported by: National Natural Science Foundation of China (51107145)

Authors: YAN Hui, male, born in 1978, Ph.D., lecturer. Research interests: sensor technologies and electromagnetic field theory and applications. E-mail: yanhui@163.com

ZHOU Guohua, male, born in 1981, Ph.D., associate professor. Research interests: military marine electromagnetic field application technologies. E-mail: dandanqibing@126.com

***Corresponding author**: ZHOU Guohua

plementary measurements at two places. Later, Xiao et al. [5] proposed the 8-shaped heading method. It requires the ship to perform a heading-changing maneuver with a large rudder angle at a high speed in the measurement site with a known geomagnetic field to cause a large change in the ship's attitude and needs plenty of effective magnetic field measurement data as support. Yan et al. [6] conducted an experimental simulation of the measurement process of the shipboard three-component geomagnetic field and found that it is difficult to measure a ship's magnetization parameters even under laboratory conditions. Therefore, the measurement of a ship's magnetization parameters is the difficulty that limits the large-scale engineering application of shipboard three-component geomagnetic field measurement systems.

To reduce the engineering difficulty and cost of measuring a ship's magnetization parameters, this paper analyzes and addresses the interference of a ship's magnetizing field with the mathematical model of a shipboard three-component geomagnetic field measurement system. Firstly, the state space equation applicable to the measurement of a ship's magnetization parameters is re-established by the Kalman filtering method used for computing the three-component geomagnetic field [3]. The paper proposes an adaptive algorithm utilizing the Kalman filtering method to solve the magnetization parameters and verifies the theoretical correctness of the algorithm by computer simulation. Then, simulated measurements are carried out in the laboratory. The magnetization parameters obtained from the solution are applied to effectively exclude the interference of the ship's magnetizing field under the condition of limited measurement data samples so that the three-component geomagnetic field can be separated precisely. This research can provide an efficient and low-cost feasible approach to the measurement of a ship's magnetization parameters.

1 Mathematical model of three-component geomagnetic field measurement

As a sensitive element to a magnetic field, a three-component magnetic sensor can collect various vector-synthesized magnetic fields at its location, including both the geomagnetic field and the magnetizing field interference from the measuring ship. The dynamic output 3 × 1 vector $\boldsymbol{B}$ of the three-component magnetic sensor mounted on the ship mast is as follows [4].

$$\boldsymbol{B} = \boldsymbol{K} \cdot \boldsymbol{A}\boldsymbol{B}_{\mathrm{e}} + \boldsymbol{B}_{\mathrm{p}} \tag{1}$$

where $\boldsymbol{K}$ is the 3 × 3 induced magnetization parameter matrix [7]; $\boldsymbol{A}$ is the transformation matrix between the 3 × 3 geographic coordinate system and the ship's coordinate system [8-9], and the matrix element is the function of measuring the attitude angle of the ship; $\boldsymbol{B}_{\mathrm{e}}$ is a 3 × 1 three-component geomagnetic field vector, nT; $\boldsymbol{B}_{\mathrm{p}}$ is a 3 × 1 fixed magnetization parameter vector [10], nT. Herein,

$$\boldsymbol{A} = \begin{bmatrix} \cos\varphi & 0 & \sin\varphi \\ 0 & 1 & 0 \\ -\sin\varphi & 0 & \cos\varphi \end{bmatrix} \begin{bmatrix} 1 & 0 & 0 \\ 0 & \cos\theta & \sin\theta \\ 0 & -\sin\theta & \cos\theta \end{bmatrix} \begin{bmatrix} \cos\psi & \sin\psi & 0 \\ -\sin\psi & \cos\psi & 0 \\ 0 & 0 & 1 \end{bmatrix} \tag{2}$$

where φ, θ, and ψ are the heading angle, roll angle, and trim angle of the ship, respectively, and they can be measured in real time by the ship's navigation system.

According to Equation (1), if the geomagnetic field $\boldsymbol{B}_{\mathrm{e}}$ needs to be separated from the measurement data of the sensor output $\boldsymbol{B}$, the ship's magnetization parameters $\boldsymbol{K}$ and $\boldsymbol{B}_{\mathrm{p}}$ must be measured first. Expanding and organizing Equation (1), one can obtain the arbitrary output component of the sensor under different ship attitudes:

$$\begin{aligned} B_i = k_{i1} f_1(\boldsymbol{B}_{\mathrm{e}}, \varphi, \theta, \psi) + k_{i2} f_2(\boldsymbol{B}_{\mathrm{e}}, \varphi, \theta, \psi) + \\ k_{i3} f_3(\boldsymbol{B}_{\mathrm{e}}, \varphi, \theta, \psi) + B_{\mathrm{p}i} \end{aligned} \tag{3}$$

where B_i is the output of the magnetic sensor in the i-th axial direction, with i = 1, 2, and 3 corresponding to the x-axis, y-axis, and z-axis, respectively; k_{i1}, k_{i2}, and k_{i3} are the elements of the first, second, and third columns in the i-th row in matrix $\boldsymbol{K}$, respectively; f_1, f_2, and f_3 are the function mapping relationships in Equation (1); $B_{\mathrm{p}i}$ is the component of the 3 × 1 fixed magnetization parameter vector $\boldsymbol{B}_{\mathrm{p}}$ in the i-th axial direction.

With a known geomagnetic field and ship attitude, at least four sets of sensor outputs at different attitudes need to be recorded to obtain the ship's magnetization parameters by solving a linear equation system. Substituting the parameters into Equation (1), one can obtain the solution of the unknown geomagnetic field $\boldsymbol{B}_{\mathrm{e}}$ as

$$\boldsymbol{B}_{\mathrm{e}} = (\boldsymbol{K}\boldsymbol{A})^{-1}(\boldsymbol{B} - \boldsymbol{B}_{\mathrm{p}}) \tag{4}$$

Although the above-mentioned computation process of the geomagnetic field holds theoretically, it is difficult to guarantee computational accuracy in practical engineering applications mainly because of the following reasons: 1) Three-component fluxgate sensors generally have inherent electrical error of null position, scale error, and quadrature error [11]; 2) in terms of ship attitude angles φ, θ, and ψ, the data are mainly from the navigation system, where drift errors exist, and there are delay errors in the signal transmission process; 3) the magnetic interference of the background environment and the quiet daily variation of the geomagnetic field can lead to a random error of the magnetic sensor [12]. Since the ship's magnetization parameters are sensitive to the above various error sources, these errors can be accumulated during the measurement process and then transferred to the geomagnetic field solution value through Equation (4). At present, there is no good method to deal with the other two types of errors except for the first one. Therefore, for improving the computational accuracy of the three-component geomagnetic field, it is necessary to adopt corresponding measures to eliminate the measurement error of the ship's magnetization parameters, so as to improve the accuracy of the mathematical model of Equation (1). The Kalman filtering method, which is widely used in dynamic measurement systems, can effectively suppress the system measurement error in principle [3,13]. Meanwhile, it can update the changing state in time through the introduction of information. When Kalman filtering is applied to the measurement of magnetization parameters, the magnetization parameters must be used as the quantities of state. However, the state is relatively invariant [4], as a result of which the measurement of the magnetization parameters has the characteristics of a static measurement system. If the static system is regarded as a special case of the dynamic system, Kalman filtering can provide a new path to measure a ship's magnetization parameters.

2 Kalman filtering algorithm

2.1 Algorithm principle

The Kalman filtering algorithm is based on the time-discretized state space of the system [14]. In the case that the ship structure and the mounted position of the magnetic sensor are unchanged, the ship's magnetization parameters $\boldsymbol{K}$ and $\boldsymbol{B}_\mathrm{p}$ are both invariants in the time domain. When the 4 × 3 extended matrix $\boldsymbol{x} = [\boldsymbol{K}\ \boldsymbol{B}_\mathrm{p}]^\mathrm{T}$ (T represents the transposition of the matrix) is used as the quantity of state, the computation equation of the measurement process is

$$\boldsymbol{x}(n+1) = \boldsymbol{x}(n) + \boldsymbol{v}_1(n) \tag{5}$$

where $\boldsymbol{x}(n)$ is the quantity of state, and the number n of measurement points equals 0, 1, 2, ..., N, with N as the maximum number of measurement points; the 4 × 3 vector $\boldsymbol{v}_1(n)$ is the process noise vector, which is used to describe the state transition error.

According to Equation (1), the observation equation can be established:

$$\boldsymbol{y}(n) = \boldsymbol{C}(n)\boldsymbol{x}(n) + \boldsymbol{v}_2(n) \tag{6}$$

where the 3 × 1 vector $\boldsymbol{y}(n) = \boldsymbol{B}^\mathrm{T}$, 1 × 4 vector $\boldsymbol{C}(n) = [\boldsymbol{B}_\mathrm{e}^\mathrm{T}\boldsymbol{A}^\mathrm{T}\ 1]$, and 3 × 1 vector $\boldsymbol{v}_2(n)$ are the observation noise vectors, which are used to describe random noise.

The state space is constituted by Equation (5) and Equation (6), and the steps of the adaptive Kalman filtering iteration algorithm are as follows:

1) Setting the initial conditions: state $\boldsymbol{x}(0)$ and intermediate variable $\boldsymbol{P}(0)$ (4 × 4 diagonal matrix).

2) Known parameters: 4 × 4 process noise variance matrix $\boldsymbol{Q}$ and one-dimensional observation noise variance $\boldsymbol{\sigma}^2$.

3) Inputs: $\boldsymbol{y}(n)$ and $\boldsymbol{C}(n)$.

4) Calculating the intermediate quantity and the quantity of state, where $\boldsymbol{R}(n)$, $\boldsymbol{P}(n)$, and $\boldsymbol{m}(n)$ are intermediate variables, and $\boldsymbol{E}$ is the identity matrix.

(1) $\boldsymbol{R}(n) = \boldsymbol{P}(n-1) + \boldsymbol{Q}$

(2) $\boldsymbol{m}(n) = \boldsymbol{R}(n)\boldsymbol{C}(n)^\mathrm{T}[\boldsymbol{C}(n)\boldsymbol{R}(n)\boldsymbol{C}(n)^\mathrm{T} + \boldsymbol{\sigma}^2]$

(3) $\boldsymbol{P}(n) = [\boldsymbol{E}-\boldsymbol{m}(n)\boldsymbol{C}(n)]\boldsymbol{R}(n)$

(4) $\boldsymbol{x}(n) = [\boldsymbol{E}-\boldsymbol{m}(n)\boldsymbol{C}(n)]\boldsymbol{x}(\boldsymbol{n}-1) + \boldsymbol{m}(n)\boldsymbol{y}(n)$

$\boldsymbol{x}(n)^\mathrm{T}$, a quantity of state, can be obtained through the above algorithm. The first three columns can constitute the induced magnetization parameter matrix $\boldsymbol{K}$, while the fourth column can form the fixed magnetization parameter vector $\boldsymbol{B}_\mathrm{p}$. In the above iteration process, the setting of the initial conditions is arbitrary to some extent. Under the condition of insufficient prior information of the state, the initial state $\boldsymbol{x}(0)$ takes zero as its value, while the initial value of the intermediate variable $\boldsymbol{P}(0)$ is assigned a small value, which is conducive to the convergence of the iteration process. As known parameters, the values of the process noise variance matrix $\boldsymbol{Q}$ and the observed noise $\boldsymbol{\sigma}^2$ play a decisive role in the convergence speed and convergence stability of the iteration process: When these two parameters have large values, the convergence is fast, while the stability is poor; conversely, the convergence is slow, while the stability is good. Therefore, in this paper, the parameter values are balanced and determined by simulation and trial computation.

2.2 Algorithm simulation

To verify the correctness of the algorithm in Section 2.1 and its ability to suppress random errors, we conduct simulation and trial computation. The three-component geomagnetic field vector is set as $\boldsymbol{B}_{\mathrm{e}}$ = [34 000, 2 000, 35 000] nT, the induced magnetization parameter matrix $\boldsymbol{K}$ = [k_{11}, k_{12}, k_{13}; k_{21}, k_{22}, k_{23}; k_{31}, k_{32}, k_{33}] = [0.95, −0.003, 0.003; 0.003, 0.95, −0.03; 0.03, −0.03, 1.05], and the fixed magnetization parameter vector $\boldsymbol{B}_{\mathrm{p}}$ = [1 500, −800, 1 800] nT. The values of ship attitude angles φ, θ, and ψ are taken from the intervals [0°, 360°], [−20°, 20°], and [−15°, 15°], respectively, and the transformation matrix $\boldsymbol{A}$ is generated. Twelve sets of sensor output vectors $\boldsymbol{B}$ are generated according to Equation (1), and the random error with the maximum value of 100 nT is applied. The values of φ, θ, and ψ corresponding to each set of vectors $\boldsymbol{B}$ are recorded, and the random error with the maximum value of 0.05° is applied. The data can be extended for multiple times of reuse, so as to ensure that the algorithm has enough iteration steps. At this time, $\boldsymbol{K}$ and $\boldsymbol{B}_{\mathrm{p}}$ can be computed according to the Kalman filtering algorithm in Section 2.1 with $\boldsymbol{B}_{\mathrm{e}}$, $\boldsymbol{A}$, and $\boldsymbol{B}$ as known quantities. The convergence of the algorithm is shown in Fig. 1.

The Kalman filtering algorithm can achieve convergence after about 300 iterations and has good stability (Fig. 1). Since random errors are applied in the simulation process in this paper, the solution is

$$\boldsymbol{K}=\begin{bmatrix} 0.949\,9 & -0.003\,6 & 0.003\,0 \\ 0.002\,7 & 0.950\,2 & -0.030\,3 \\ 0.029\,5 & -0.029\,6 & 1.049\,9 \end{bmatrix}$$

$$\boldsymbol{B}_{\mathrm{p}}=[1\,497 \quad -809 \quad 1\,806]\ \mathrm{nT}$$

Compared with the set value, $\boldsymbol{K}$ and $\boldsymbol{B}_{\mathrm{p}}$ have errors at the 0.000 1 and 1 levels, respectively. Given that the geomagnetic field is at the level of 10^4 nT, the error is estimated according to the transfer relationship of Equation (3). Thus, the computational error of the geomagnetic field due to the measurement error of the ship's magnetization parameters is approximately at the level of 10 nT, which is equivalent to the computational error level of the geomagnetic field obtained by only considering the random measurement error in Reference [3].

3 Mockup verification experiment

3.1 Experimental model and measurement process

To test the validity of the Kalman filtering method in the measurement of the ship's magnetization parameters, we conduct the validation experiment on a mockup in a non-magnetic laboratory. The measuring device consists of a three-component fluxgate sensor, a horizontal angle sensor, and a rig-

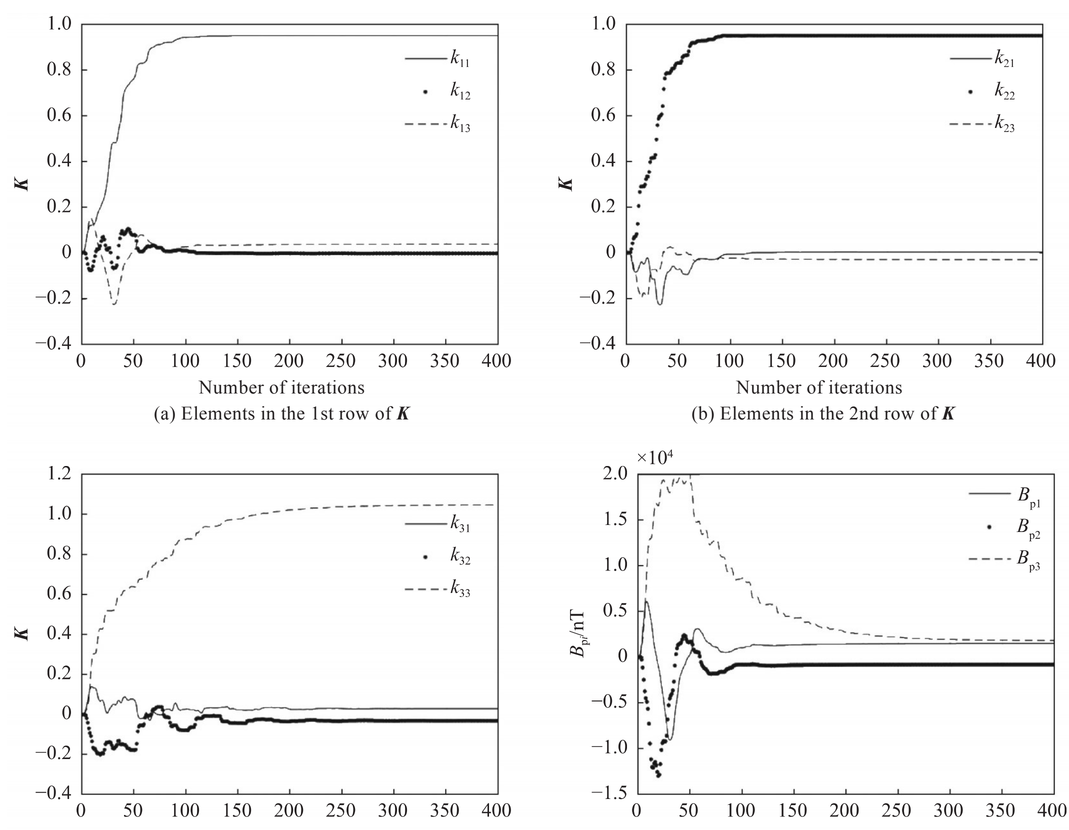

(a) Elements in the 1st row of $\boldsymbol{K}$ (b) Elements in the 2nd row of $\boldsymbol{K}$

(c) Elements in the 3rd row of $\boldsymbol{K}$ (d) Three elements of $\boldsymbol{B}_{\mathrm{p}}$

Fig. 1 Convergence curves of magnetization parameters in simulation id non-magnetic stainless steel bracket. The magnetic sensor and the angle sensor are rigidly connected through the bracket. Attention should be paid to adjusting the corresponding measuring shaft. The measuring device is installed on a magnetic mockup, and the measuring shaft is consistent with the ship's coordinate system (Fig. 2). The magnetic mockup is placed on a non-magnetic platform, which can meet the rotation, rolling, and trim requirements of the mockup in four main headings. In this way, the shipboard three-component geomagnetic field measurement platform can be constructed.

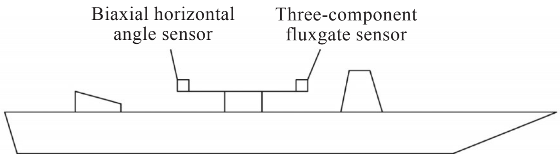

Fig. 2 Experiment device

For the sake of simplifying the measurement process, magnetic interference measurement is conducted on the mockup under three horizontal attitudes in four main headings of magnetic east, magnetic north, magnetic west, and magnetic south. A total of 12 sets of measurement data are obtained, and the measurement data of the three-component magnetic sensor and horizontal angle sensor are recorded simultaneously.

3.2 Measurement results and calculation analysis

The measurement data are shown in Table 1, where the three components of the magnetic sensor, roll angle, and trim angle are the measured values of the sensor, while the four heading angles of magnetic east, magnetic north, magnetic west, and magnetic south are directly assigned as 90°, 0°, 270°, and 180° and converted into radians.

Under the known ambient geomagnetic field $\boldsymbol{B}_e$ = [34 425, 1 961, 35 898] nT, $\boldsymbol{K}$ and $\boldsymbol{B}_p$ can be obtained by the above-mentioned Kalman filtering algorithm:

The induced magnetization parameter matrix is

$$\boldsymbol{K}=\begin{bmatrix} 0.985\,75 & 0.081\,53 & 0.062\,21 \\ -0.062\,33 & 0.835\,17 & -0.029\,87 \\ -0.029\,99 & -0.077\,48 & 1.066\,15 \end{bmatrix},$$

The fixed magnetization parameter vector is

$\boldsymbol{B}_p$ = [2 011.1, −2 886.8, 2 054.6] nT.

Due to the extra small data volume of the measurement (only 12 sets), the number of iteration steps of the filter is too small to converge. To solve this problem, this paper extends the 12 sets of data, namely that the 12 sets of data are reused multiple times, and they serve as the experimental data set. The magnetization parameters can be computed by extracting a certain amount of data from the experimental data set. Fig. 3 shows the iteration process curves of the induced magnetization parameter and the fixed magnetization parameter.

For the case of a small amount of measurement data, the Kalman filtering algorithm still presents good convergence by the repeated extension of the data (Fig. 3). However, compared with the simulation results, the experimental results see slightly decreased stability after convergence with slight fluctuations. The data used in the simulation are ideal values without errors, while the magnetic field, heading angle, roll angle, and trim angle measured by the sensor in the experiment have errors. There-

Table 1 Measured magnetic field data of the mockup

Parameter number	Three components of magnetic sensor			Heading angle ψ/rad	Roll angle θ/rad	Trim angle φ/rad
	B_1 /nT	B_2 /nT	B_3 /nT			
1	4 206	25 290	36 913	4.712 39	0.025 22	−0.004 26
2	−30 595	−2 785	40 620	3.141 59	0.024 73	−0.003 02
3	2 478	−31 825	43 890	1.570 80	0.023 21	−0.002 62
4	37 118	−3 690	40 110	0.000 00	0.023 09	−0.003 91
5	37 485	−9 719	39 480	0.000 00	−0.174 01	−0.014 15
6	2 608	−36 985	36 580	1.570 80	−0.173 47	−0.012 90
7	−30 197	−8 205	41 110	3.141 59	−0.171 83	−0.013 28
8	4 761	19 020	43 985	4.712 39	−0.171 27	−0.014 54
9	37 811	2 408	37 845	0.000 00	0.222 70	−0.021 92
10	4 514	30 860	28 158	4.712 39	0.224 57	−0.022 46
11	−29 836	3 038	39 796	3.141 59	0.223 66	−0.022 48
12	3 615	−25 322	49 387	1.570 80	0.222 16	−0.022 11

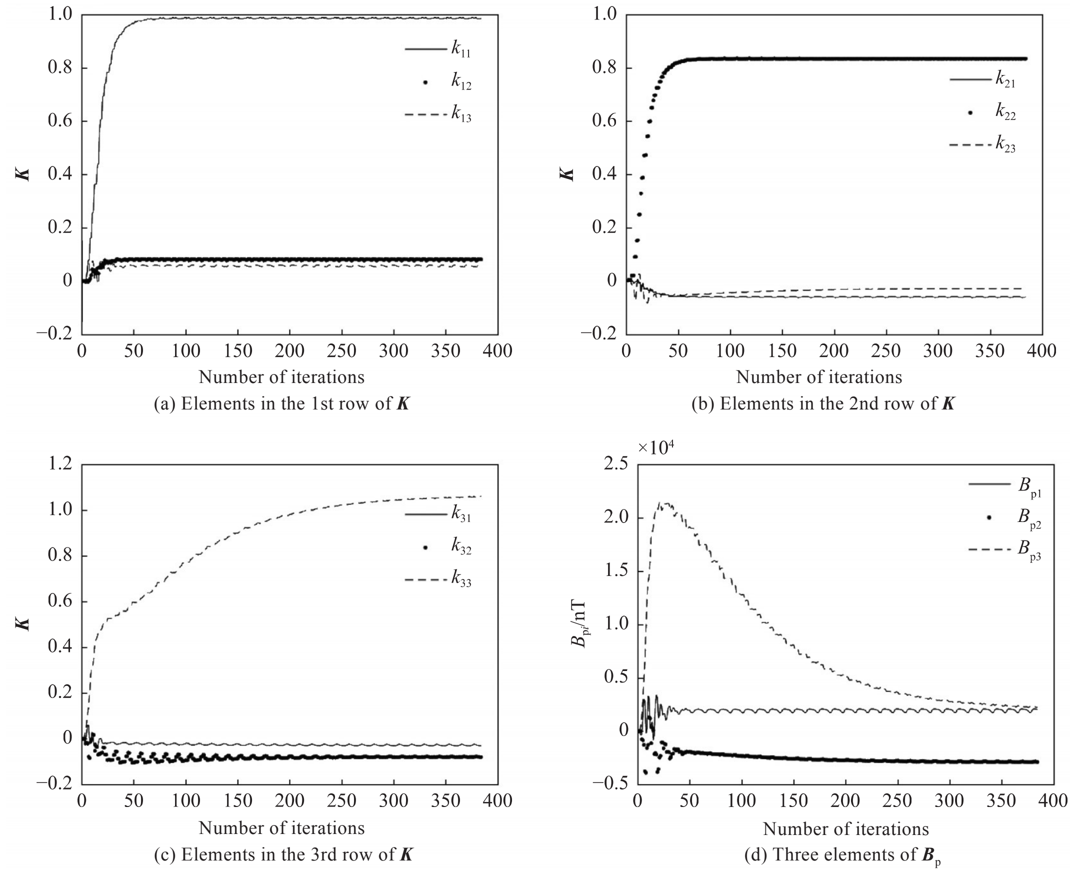

(a) Elements in the 1st row of $\boldsymbol{K}$ (b) Elements in the 2nd row of $\boldsymbol{K}$

(c) Elements in the 3rd row of $\boldsymbol{K}$ (d) Three elements of $\boldsymbol{B}_p$

Fig. 3 Convergence curves of magnetization parameters in experiment

fore, the main reason for the stability decline is the measurement error of the experimental data.

To verify the correctness of the ship's magnetization parameters in Table 1, we substitute them into the three-component geomagnetic field computation algorithm in Reference [3] and extract some data samples from the experimental data set for geomagnetic field computation. The convergence process is shown in Fig. 4, where B_{ei} is the component of the 3 × 1 three-component geomagnetic field vector $\boldsymbol{B}_e$ in the i-th axial direction (i = 1, 2, and 3). According to the computational results, the maximum relative error of the stable geomagnetic field solution data after convergence is 1.9% (defined as the

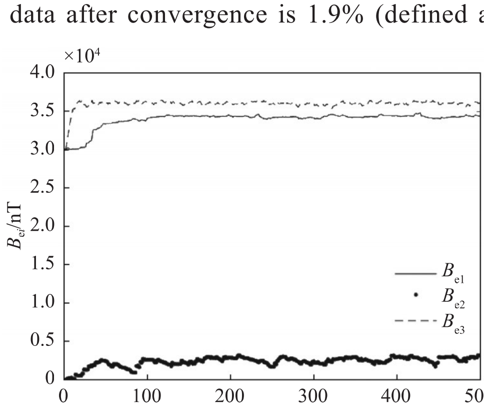

Fig. 4 The convergence curves in computing three-component geomagnetic field

ratio of the maximum error to the total geomagnetic field), and the root mean square error is 266 nT. To sum up, the Kalman filtering algorithm not only has high computational accuracy but also possesses the ability to suppress measurement error under the condition of only 12 sets of measurement data.

4 Conclusions

In the shipboard three-component geomagnetic field measurement system, the core issue is the measurement of the ship's magnetization parameters. This paper proposes the measurement algorithm of a ship's magnetization parameters based on the Kalman filtering method. Depending on the mathematical model of the sensor measurement output of the shipboard three-component geomagnetic field measurement system, the observation equation can be established. According to the relative invariance of the ship's magnetization parameters, the process equation can be established. The state space expression composed of the observation equation and the process equation can well meet the stringent requirements of Kalman filtering for model accuracy, and the theoretical correctness of the algorithm is verified by computer simulation. With limited experimental data samples, the good convergence of the Kalman filtering algorithm can be ensured by simply reusing the data. Compared with the "four-heading method," the Kalman filtering method can measure all the magnetization parameters without the need to strictly adhere to the measurement in the four main headings of east, west, south, and north. Compared with the 8-shaped heading method, the proposed method requires less data and does not require measurement on a specific track. Therefore, considering the completeness of magnetization parameter measurement, the required data volume, and the difficulty in creating the measurement implementation conditions, the Kalman filtering method can significantly improve the measurement efficiency for a ship's magnetization parameters and reduce the difficulty in engineering implementation.

During the measurement simulation in the laboratory, the main reasons affecting the measurement accuracy are as follows: The inherent errors of the three-component magnetic sensor are not corrected; there are measurement errors in the ambient geomagnetic field when magnetization parameters are measured; there are sensor installation errors, especially the consistency error between the x-axis direction of the sensor and the direction of the fore-and-aft line; the angle sensor can only measure the roll angle and trim angle, and the heading angle is only approximated using the laboratory orbital direction. Therefore, in practical engineering applications, these errors need to be further dealt with to improve the measurement accuracy of a ship's induced magnetization parameters.

References

[1] MACBAIN J A. Some aspects of vehicle degaussing [J]. IEEE Transactions on Magnetics, 1993, 29(1):159−165.

[2] NORGREN M, HE S L. Exact and explicit solution to a class of degaussing problems [J]. IEEE Transactions on Magnetics, 2000, 36(1): 308−312.

[3] YAN H, XIAO C H, SU G D. Application of multimodel Kalman filtering in surveying marine geomagnetic field [J]. Science of Surveying and Mapping, 2010, 35 (1): 41−43 (in Chinese).

[4] XIAO C H. Degaussing theories and techniques used in ship's degaussing system [D]. Wuhan: Huazhong University of Science and Technology, 1999 (in Chinese).

[5] XIAO C H, ZONG S L. Simulation of S matrix measurement of ship degaussing system [J]. Journal of Naval University of Engineering, 2002, 14(4): 16−20 (in Chinese).

[6] YAN H, XIAO C H, SHEN M, et al. The algorithm verification for geomagnetic three-component computation with shipboard measurement system [J]. Hydrographic Surveying and Charting, 2010, 30(3): 27−29 (in Chinese).

[7] YANG B F, FAN B Y, XU J M, et al. Research on error compensation in geomagnetic field measurement based on least squares [J]. Journal of Air Force Engineering University (Natural Science Edition), 2017, 18 (6): 34−39 (in Chinese).

[8] PANG H F, PAN M C, QU W, et al. A new misalignment calibration method of portable geomagnetic field vector measurement system [J]. Measurement, 2020, 164: 108041.

[9] LIU Y, WANG Y T, HU X M. Study on the 3 DOF tracking algorithm to measure the motion of the rigid body [J]. Computer Measurement & Control, 2002, 10 (6): 363−365 (in Chinese).

[10] GAO J J. Research on computing induced and permanent magnetic field of large asymmetric ships [D]. Wuhan: Naval University of Engineering, 2008 (in Chinese).

[11] SUN H, YANG B F, GUAN H, et al. Calibration of three-axis fluxgate magnetometers with joint estimation iterative algorithm [J]. Acta Armamentarii, 2020, 41(5): 902−910 (in Chinese).

[12] REN L P, ZHANG X A, LIU G B. Research for source of systematic error in marine magnetic survey [J]. Hydrographic Surveying and Charting, 2004, 24(5): 5−8 (in Chinese).

[13] WANG Y, DE-SILVA C W. Sequential Q-learning with Kalman filtering for multirobot cooperative transportation [J]. IEEE/ASME Transactions on Mechatronics, 2010, 15(2): 261−268.

[14] ZHANG X D. Modern signal processing [M]. Beijing: Tsinghua University Press,2002:157−188 (in Chinese).

基于Kalman滤波的船舶磁化干扰系数测量算法

闫辉[1], 周国华[*2]

1 信阳学院 大数据与人工智能学院,河南 信阳 464000

2 海军工程大学 电气工程学院,湖北 武汉 430033

摘　要:［**目的**］针对以船舶为载体的三分量地磁场测量系统,为了提高其测量效率并降低工程难度,提出基于Kalman滤波的船舶磁化干扰系数测量算法。［**方法**］根据三分量地磁场测量数学模型中船磁干扰的作用形式及特征,提出解算船舶磁化干扰系数的Kalman滤波算法实施步骤,然后开展计算机仿真和船模实验,以验证该算法的有效性。［**结果**］在有效磁场测量数据样本较少的条件下,该算法保证了良好的收敛性,分离出了较高精度的三分量地磁场。［**结论**］Kalman滤波算法为船舶磁化干扰系数测量的工程实践提供了一条高效率、低成本的可行路径。

关键词:三分量地磁场;舰船磁场;Kalman滤波;磁防护